

A New Horizontal Polarized High Gain Omni-Directional Antenna

Tom presents a helical antenna design that produces significantly horizontally polarized gain.

Background

High gain omni-directional antennas are more difficult to realize with horizontal polarization. Vertical radiating elements stacked along a vertical line provide a natural means of achieving high gain with vertical polarization. Radiating elements are often $\lambda/2$ or near $\lambda/2$. When these elements are rotated to a horizontal mode, the familiar bidirectional dipole azimuth pattern is seen. Turnstile arrays were early answers to the challenge of omni-directional performance with horizontal polarization.^{1,2} Dipoles also have been wrapped into circular (Halo) or square (Squalo) shapes to mitigate the pattern; however, gain is reduced.³ Perhaps the best implementation of circularly wrapped dipoles is the Big Wheel where three dipoles form a circular array.⁴ An excellent printed board implementation has been done by Kent Britain, WA5VJB. Basic performance of the Halo and Big Wheel structures has been extended by use of folded dipole elements. The folded dipole Halo has been done by Delbert Fletcher, K5DDD, and

the folded dipole Super Wheel is credited to Tom Haddon, K5VH. Slots in cylinders or in rectangular wave guides have offered another approach to horizontal polarization at higher frequencies where $\lambda/2$ elements

become quite small. Figure 1 shows photos of some of these horizontally polarized omni-directional antennas. Cebik and Cerreto should also be mentioned for the three dipole array that yields a far field radi-

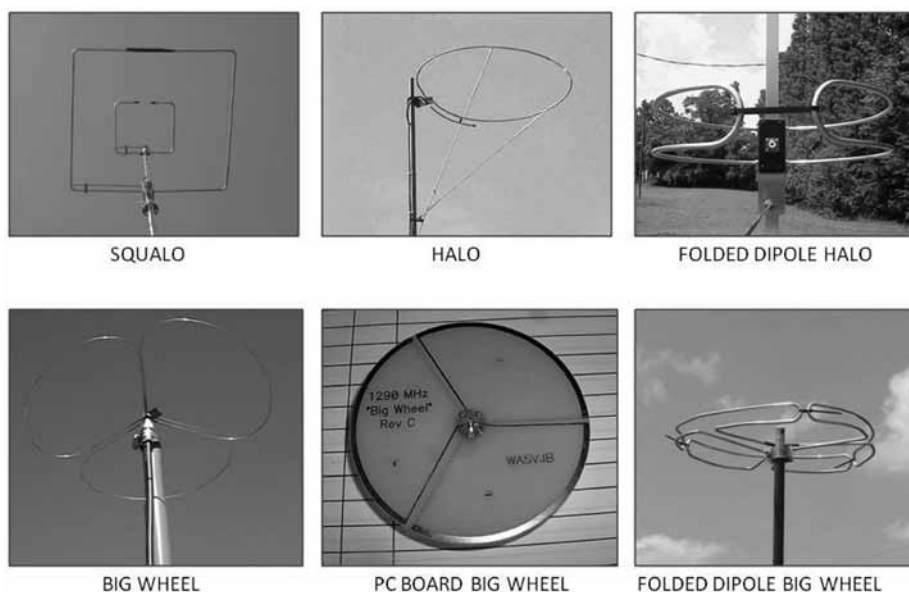


Figure 1— Photos of popular horizontal polarized omni-directional antennas

¹Notes appear on page 00.

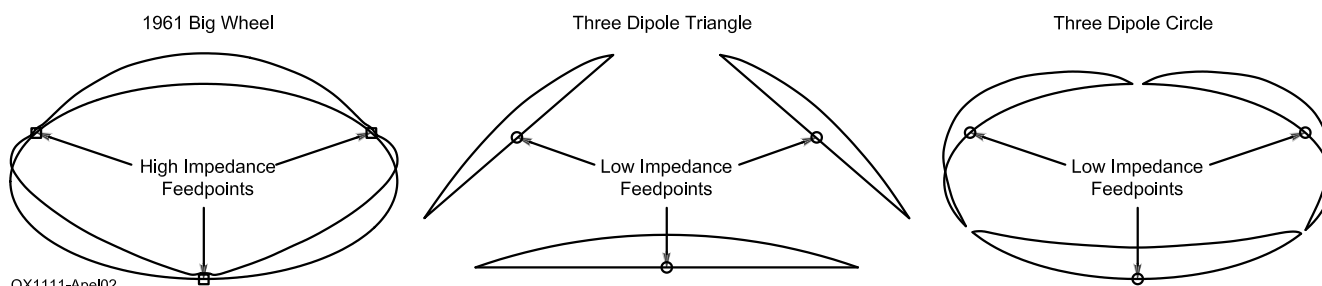


Figure 2 – Current distributions on several arrays of three half wave elements (from Cebik)

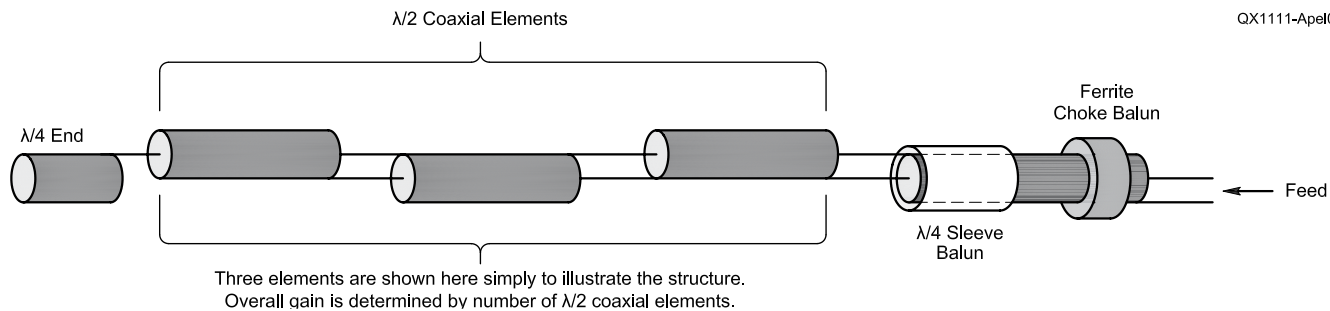
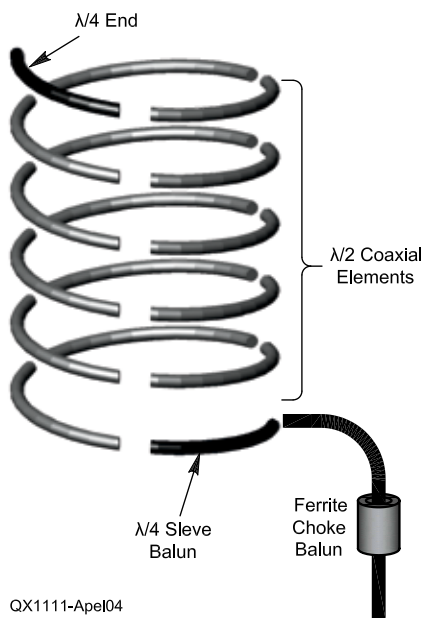
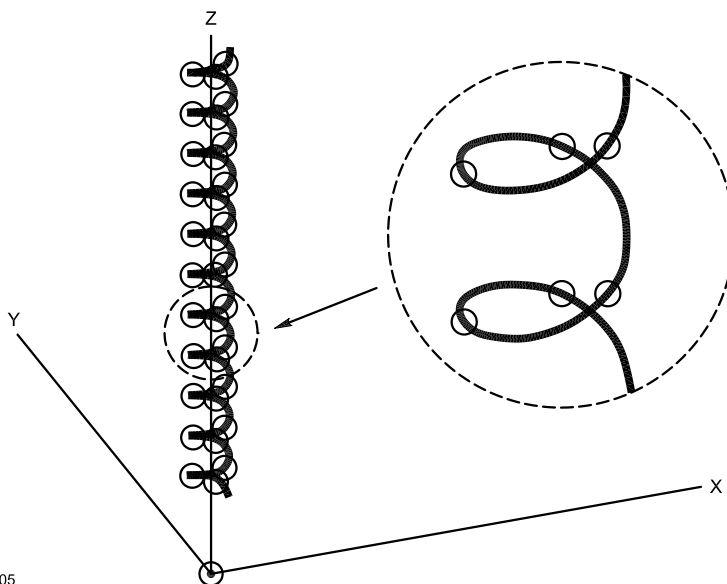


Figure 3 – Coaxial collinear structure showing the electrical connections



QX1111-Apel04

Figure 4 – Coaxial collinear structure showing the physical configuration



QX1111-Apel05

Figure 5 – EZNEC model of 11 turn helical collinear

tion pattern nearly identical to that of the Big Wheel.⁵ This is a result of the similarity in current distribution on the three dipoles to that of arrays of three dipoles around a circle as illustrated in Figure 2.

High gain requires stacking an array of horizontally polarized unit structures. The feed complexity associated with ten or twelve stacked elements is not trivial. At this point, it is noteworthy to point out the relative ease in feeding many elements in vertical collinear arrays.

The Idea

Consider the coaxial collinear structure shown in Figure 3. With the exception of the end elements, all radiating elements are comprised of $\lambda/2$ segments of coaxial cable. Each section is end fed by the previous section. Current on the shield of each coaxial

Table 1

Helical Collinear Calculations 902 MHz

	(Inches)	(mm)		
Length $\lambda/2$	4.60	116 (0.35 λ)	Elements/Turn	3
Diameter	4.10	104 (0.31 λ)	Turns	11
Pitch	4.95	126 (0.38 λ)	Total Segments	264
Linear Total	153.78	3906 (11.65 λ)	N $\lambda/2$	32
Helix Length	54.48	1384 (4.13 λ)	Segments/Turn	24
Bottom	5.91	150		
Top	60.39	1534		

section produces the desired radiation. The delay through each section must be 180° in order to properly feed the next section in the array. Hence, the length should be cut to $\lambda/2$ in the coax medium. If the $\lambda/2$ elements are wrapped around a vertical axis into a helix with three elements per turn, the resulting structure approximates the circular array comprised in stacked unit wheel structures.

Figure 4 illustrates the helical collinear structure. This approach allows many elements to be fed simply from a common point. The turn-to-turn pitch is an important design parameter. It trades off horizontal polarization “purity” with gain. The large pitch limit is, of course, the vertical collinear with no horizontal component. One expects good gain in the horizontal mode when pitch approaches $\lambda/2$.

Simulation

EZNEC was used to simulate the performance of the helical collinear.⁶ The first case considered consisted of 11 turns with a turn-pitch of 0.38λ . This model is illustrated in Figure 5. A sample model-prep calculation sheet is shown in Tables 1 and 2.

With these preliminary calculations, a helical model with periodic current sources can be constructed. The current magnitudes can also be tapered to allow for attenuation on the coaxial line segments. Azimuth and elevation simulation results are shown in Figures 6 and 7. A good omni-directional pattern is achieved with +10.6 dBi gain. This is a bit more than +8 dB over a dipole. The azimuth pattern has approximately ± 0.4 dB ripple. A larger turn pitch will reduce this but also increase the vertical polarization content.

The results from a 22 turn simulation are

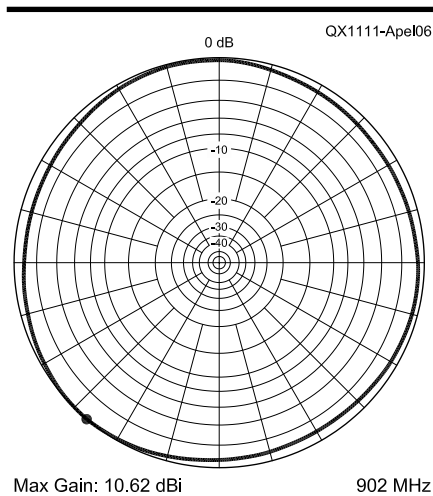


Figure 6 – EZNEC azimuth plot of 11 turn helical collinear

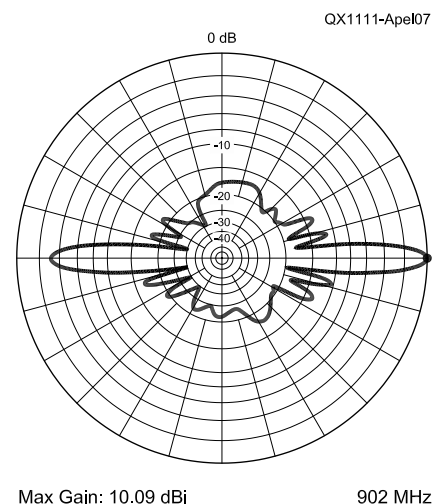


Figure 7 – EZNEC elevation plot of 11 turn helical collinear (pitch = 0.5λ)

shown in Figures 8, 9, and 10. The turn pitch for this case was approximately $\lambda/2$. This structure yields +12.2 dBi (+10 dBd) gain.

Sensitivity

The practical matter of errors in the length

of elements must be emphasized. With half wave dimensions of 4.6" in RG-316, a 2° error in the element length is represented by 50 mils. Careful measurement with a caliper can keep element length errors within an acceptable level. The worst case would be

Table 2
902 MHz EZNEC Port Definition

Element		Linear (Inches)	Linear (mm)	Z-coordinate (mm)	Segments	Bottom Segment
1	$\lambda/4$	150.48	3822	1504	4	260
2	$\lambda/2$	145.88	3705	1462	8	252
3	$\lambda/2$	141.28	3588	1421	8	244
4	$\lambda/2$	136.68	3471	1379	8	236
5	$\lambda/2$	132.08	3354	1338	8	228
6	$\lambda/2$	127.48	3237	1297	8	220
7	$\lambda/2$	122.88	3121	1255	8	212
8	$\lambda/2$	118.28	3004	1214	8	204
9	$\lambda/2$	113.68	2887	1173	8	196
10	$\lambda/2$	109.08	2770	1131	8	188
11	$\lambda/2$	104.48	2653	1090	8	180
12	$\lambda/2$	99.88	2536	1048	8	172
13	$\lambda/2$	95.28	2420	1007	8	164
14	$\lambda/2$	90.68	2303	966	8	156
15	$\lambda/2$	86.08	2186	924	8	148
16	$\lambda/2$	81.48	2069	883	8	140
17	$\lambda/2$	76.88	1952	841	8	132
18	$\lambda/2$	72.28	1835	800	8	124
19	$\lambda/2$	67.68	1719	759	8	116
20	$\lambda/2$	63.08	1602	717	8	108
21	$\lambda/2$	58.48	1485	676	8	100
22	$\lambda/2$	53.88	1368	634	8	92
23	$\lambda/2$	49.28	1251	593	8	84
24	$\lambda/2$	44.68	1134	552	8	76
25	$\lambda/2$	40.08	1017	510	8	68
26	$\lambda/2$	35.48	901	469	8	60
27	$\lambda/2$	30.88	784	427	8	52
28	$\lambda/2$	26.28	667	386	8	44
29	$\lambda/2$	21.68	550	345	8	36
30	$\lambda/2$	17.08	433	303	8	28
31	$\lambda/2$	12.48	316	262	8	20
32	$\lambda/2$	7.88	200	220	8	12
33	$\lambda/2$	3.28	83	179	8	4
34	$\lambda/4$	0.00	0	150	4	0

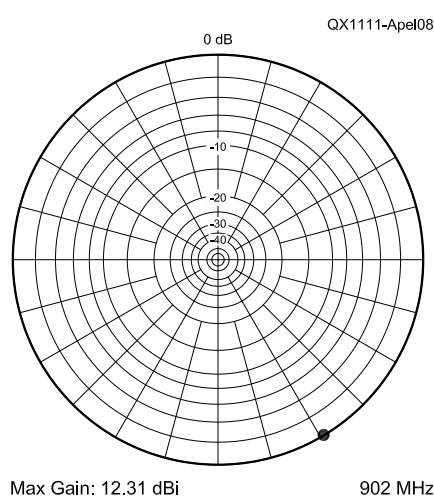


Figure 8 – EZNEC azimuth plot of 22 turn helical collinear (pitch = 0.5λ)

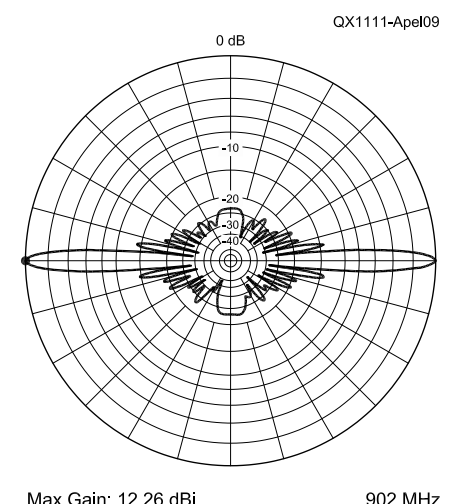


Figure 9 – EZNEC elevation plot of 22 turn helical collinear (pitch = 0.5λ)

if *all* elements were short or *all* were long. This would propagate a cumulative error throughout the array. While this is unlikely, it is a worst case worthy of analysis. Figure 11 shows a net up or down tilt in the main lobe elevation by approximately 2° , from an analysis of the 11 turn helix with a 2° error in the length of each element. Similarly, Figure 12 shows the same result from an analysis of the 22 turn helix with a 2° error in the length of each element. Practically, one would expect the elements to be constructed to the correct length in the mean, with some distribution in length errors (both short and long). This will spread the main lobe for some net loss in gain rather than a net tilt up or down.

Design Considerations

Each turn contains three $\lambda/2$ elements as in “big wheel” structures. I briefly looked at four elements per turn. My thinking was that opposing elements would be antiphased with separation near $\lambda/2$, so gain might be good. While this type of structure yields gain, it is not as good as the three elements per turn case and it has a larger diameter. It was concluded that the three elements per turn case was the best.

The most important design parameter is turn pitch. This is the vertical distance between the beginning and end of each turn in the helix. When the pitch is smaller, the larger number of turns emulates “big wheel” structures, but the stacking distance is closer. Horizontal polarization dominates and gain is poor as a result of the effective closer stacking. The other extreme is the vertical collinear when pitch approaches 1.5λ . This yields very good gain in vertical polarization only. The best stacking distance without grating lobes is $\lambda/2$. The obvious question is: How does pitch trade-off the fraction of radiated energy in the horizontal polarization? Figure 13 plots this trade-off for an 11 turn helix. These analysis results are qualitatively representative of other cases with differing number of turns. Several important observations can be made:

1. While total gain continues to increase with pitch, best gain in the horizontal polarization is achieved with pitch $\geq 0.38 \lambda$.
2. Vertical polarization is -13 dB down from total at pitch of 0.38λ . This degrades to -8 dB as the pitch is increased to $\lambda/2$.
3. Based on the above observations, the optimum pitch is 0.38λ to 0.4λ .

Driving point impedance depends on the number of elements. As the number of elements is increased, the impedance lowers. I have built prototypes for 902 MHz and 1296 MHz with 11 turns and 15 turns respectively. Both have yielded good VSWR to

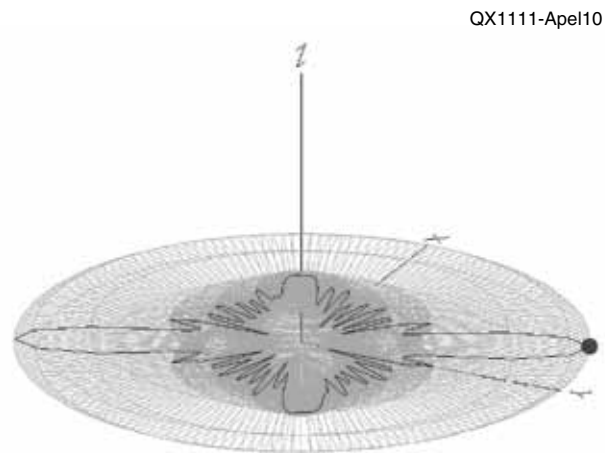


Figure 10 – EZNEC 3D plot of 22 turn helical collinear (pitch = 0.5λ)

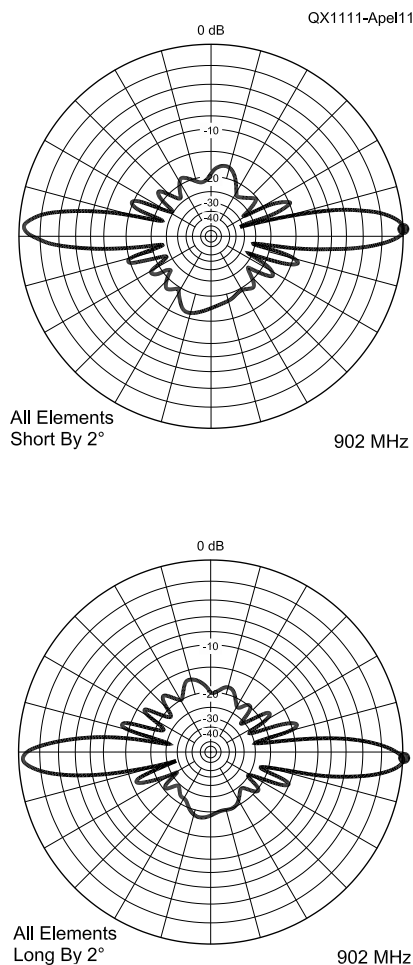


Figure 11 – EZNEC simulation of 11 turn helix with $\pm 2^\circ$ length error on ALL elements (pitch = 0.38λ). Note the upward tilt for all short and downward tilt for all long.

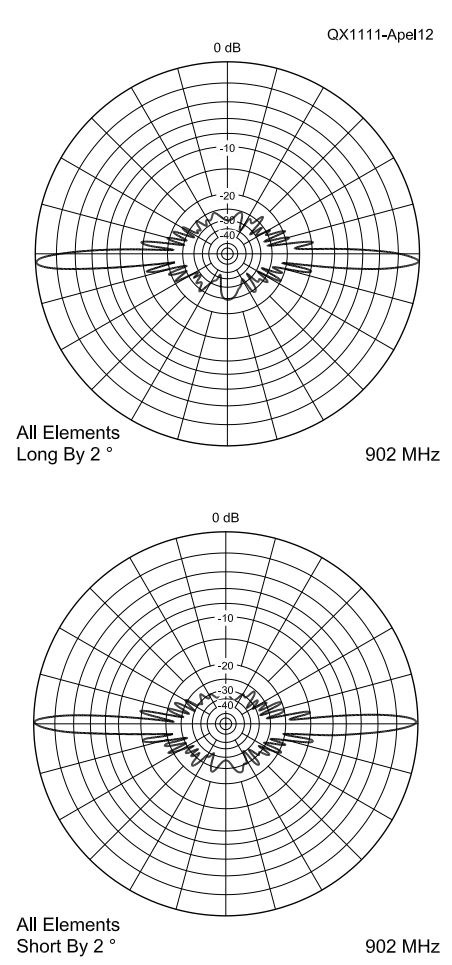


Figure 12 – EZNEC simulation of 22 turn helix with $\pm 2^\circ$ length error on ALL elements (pitch = 0.5λ)

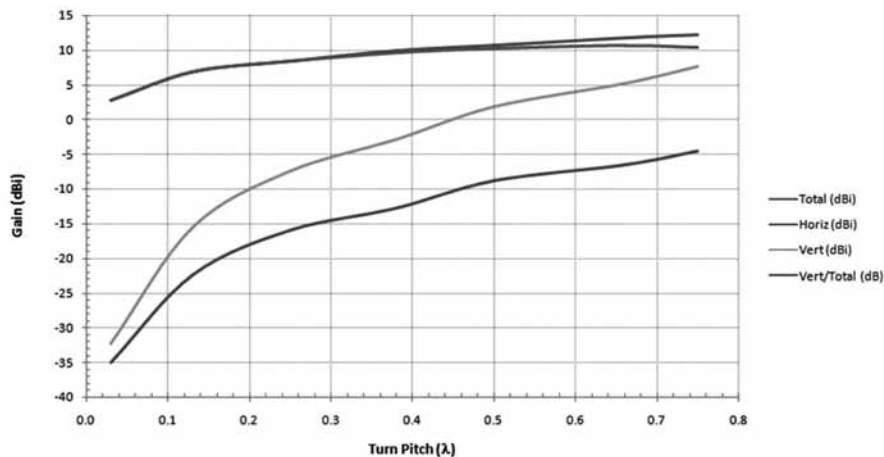


Figure 13 – Gain and polarization trade-offs with turn pitch (from 11 turn helical collinear)

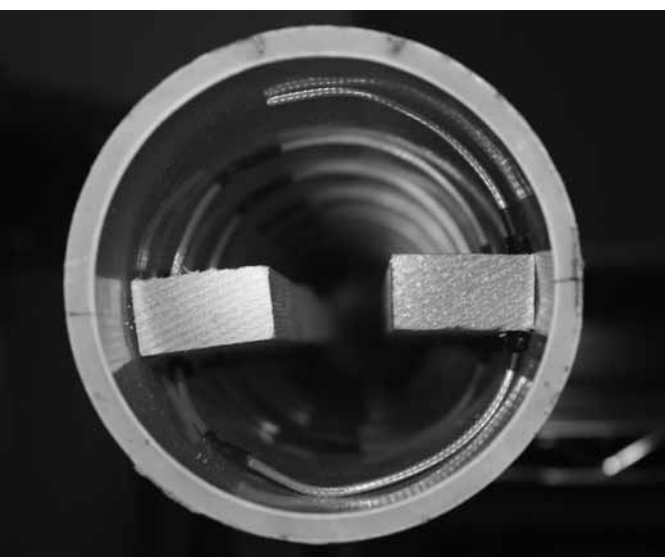


Figure 14 – Interior view of PVC with wood supports for RG316 elements (11 turn helical collinear)



Figure 15 – Completed 902 MHz helical collinear prototype

50Ω. On the other hand, I constructed a single turn “big wheel” (plus $\frac{1}{4} \lambda$ end section) with RG-8 coax for 6 meters. This required a 4:1 transformer for good VSWR.

Construction

A PVC radome can be used to enclose high frequency realizations of this antenna. For 902 MHz, 4” tubing works well. At 1296 MHz, a 3” PVC pipe yields good results. The coaxial elements are radiating due to currents on the shield. Since they are each cut to $\lambda/2$ in the coax medium, each will be less than $\lambda/2$ as a radiating element in free space. The dielectric loading effect of the PVC actually helps mitigate this.

Wood slats were inserted into the PVC tube and screwed to opposite side walls. These wooden slats form supports to attach the coaxial elements. The interior view of the 902 MHz prototype can be seen in Figure 14. The overall completed 902 MHz antenna can be seen in Figure 15.

Table 3

Helical Collinear Calculations 1296 MHz

	(Inches)	(mm)			
Length $\lambda/2$	3.20	81	(0.35 λ)	Elements/Turn	3
Diameter	2.85	72	(0.31 λ)	Turns	15
Pitch	3.46	88	(0.38 λ)	Total Segments	180
Linear Total	145.38	3693	(15.94 λ)	N $\lambda/2$	44
Helix Length	51.95	1320	(5.70 λ)	Segments/Turn	12
Bottom	5.91	150			
Top	57.85	1470			

Teflon dielectric coax such as RG400 and RG316 should be used because it can withstand soldering temperatures without shorting. The velocity factor is also a bit higher.

Assembly of the 1296 MHz prototype array onto the wooden supports can be seen in Figure 16. The supports were pre-drilled prior to assembly. During assembly, the wooden supports were ‘zip-tied’ together as shown in the figure. After all elements are arrayed along the support, the ties can be removed and the assembly can be inserted

into the PVC tube. Heat shrink tubing was also used to cover and reinforce each junction. For additional mechanical support, short lengths of Tygon or Excelon fuel line tubing can be placed over the heat shrink tubing. For RG-316, I have used tubing with 3/16” OD and 3/32” ID. At 902 and 1296 MHz, it is critical to keep the element to element transitions extremely short. Parasitic inductance can have a significant cumulative effect on performance. Proper element length is also critical. As discussed previously, a

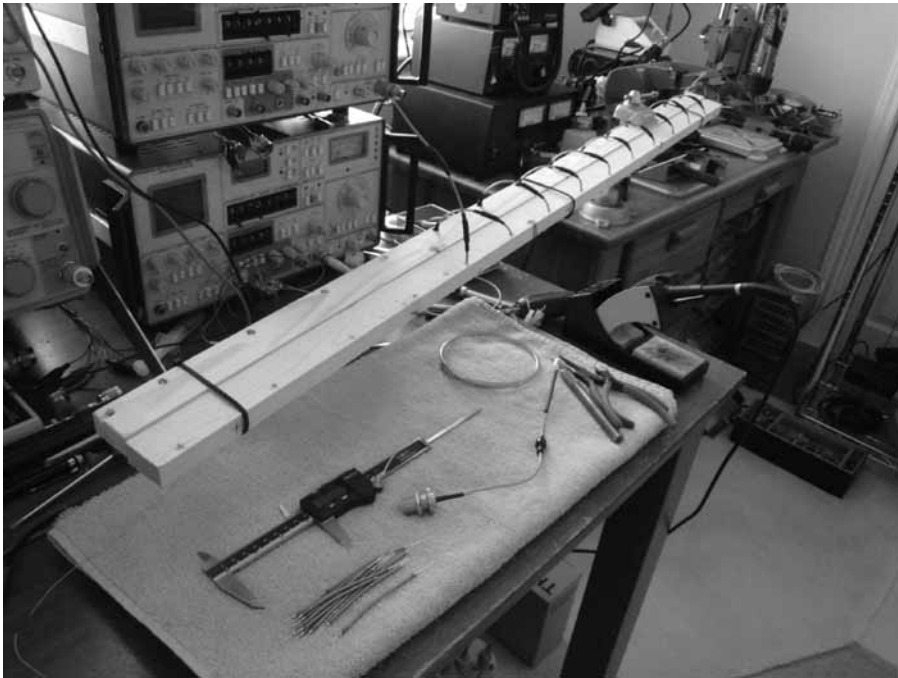


Figure 16 – Assembly of 1296 MHz elements on wood supports

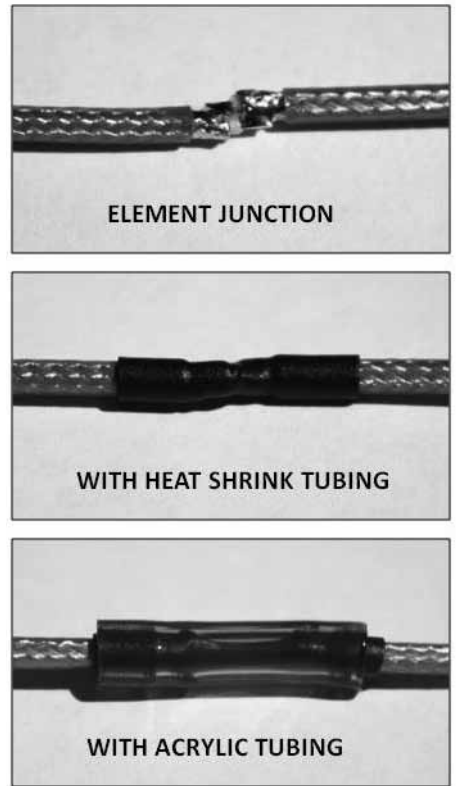


Figure 17 – Construction of element junctions



Figure 18 – Completed 1296 MHz helical collinear prototype

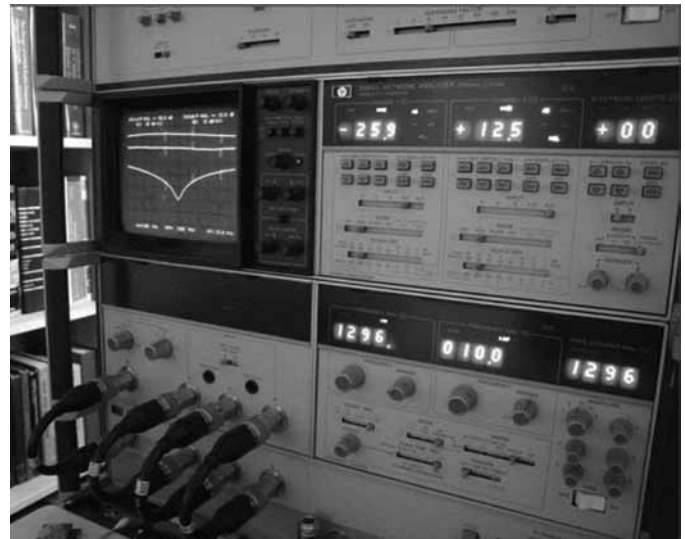


Figure 19 – Measured comparison with 1296 MHz “big wheel”

50 mil error in element length can introduce a 2° error in the element length. Elements are best pre-cut using dial or digital calipers. A detailed view of the construction of a junction of elements is shown in Figure 17. For lower frequencies where PVC tubing is not practical in the necessary dimensions, a turnstile support framework is suggested.

The completed 15 turn 1296 MHz antenna is shown in Figure 18. See Tables 3 and 4 for a sample model calculation sheet.

Conclusions

To date, prototype antennas of this type have been constructed and tested for 1296 MHz, 902 MHz, and 50 MHz, although the 50 MHz case was only a single turn. Good results have been obtained in each case. In an attempt to make a measurement of the gain relative to a Big Wheel, a reference path was established between two Big Wheels and then one was replaced by the 15 turn 1296 MHz helical collinear. The network analyzer display of this measurement can be seen in Figure 19. The two horizontal traces on the CRT display the pair of |S21| responses (10 dB/division). I must say that this was not performed on a good antenna range. I am sure reflections were causing errors, so the +12.5 dB gain over a single Big Wheel is likely optimistic. On the other hand, it is safe to say that the omni-directional gain offered from this type of structure is quite good. The ease of feeding the array from a single point is also a very significant advantage.

Tom Apel is an electrical engineer. He retired in 2010 from Triquint Semiconductor as Senior Engineering Fellow where he managed advanced component development. Mr. Apel has 33 years in microwave and RF component design at VHF through Ka band. He developed the first 6-18 GHz 2W power amplifier MMIC to achieve volume production. More recently, his work has resulted in many power amplifier products for handset applications. During his career he was responsible for 34 US Patents. He earned a BS Physics and BS Mathematics from Loras College, and MSE from University of Wisconsin, Madison. Tom was first licensed in 1963 and has been home brewing since then.

Notes

- ¹G.H Brown, "The Turnstile Antenna" *Electronics*, April 1936.
- ²D.W. Masters, "The Super-turnstile Antenna" *Broadcast News*, January 1946.
- ³F.H. Stites, W1MUX/3, "A Halo for Six Meters" *QST*, October 1947.
- ⁴R.H. Mellen, W1UD, and C. T. Milner, W1FVY, "The Big Wheel on Two" *QST*, September 1961.
- ⁵L.B. Cebik, W4RNL, and R. Cerreto, WA1FXT, "A New Spin on the Big Wheel" *QST*, March 2008.
- ⁶EZNEC software available from developer Roy Lewallen, W7EL at www.ez nec.com.

Table 4
1296 MHz EZNEC Port Definition

Element	Linear (Inches)	Linear (mm)	Z-coordinate (mm)	Segments	Bottom Segment
1	$\lambda/4$	143.10	3635	2	178
2	$\lambda/2$	139.90	3553	4	174
3	$\lambda/2$	136.70	3472	4	170
4	$\lambda/2$	133.50	3391	4	166
5	$\lambda/2$	130.30	3310	4	162
6	$\lambda/2$	127.10	3228	4	158
7	$\lambda/2$	123.90	3147	4	154
8	$\lambda/2$	120.70	3066	4	150
9	$\lambda/2$	117.50	2984	4	146
10	$\lambda/2$	114.30	2903	4	142
11	$\lambda/2$	111.10	2822	4	138
12	$\lambda/2$	107.90	2741	4	134
13	$\lambda/2$	104.70	2659	4	130
14	$\lambda/2$	101.50	2578	4	126
15	$\lambda/2$	98.30	2497	4	122
16	$\lambda/2$	95.10	2415	4	118
17	$\lambda/2$	91.90	2334	4	114
18	$\lambda/2$	88.70	2253	4	110
19	$\lambda/2$	85.50	2172	4	106
20	$\lambda/2$	82.30	2090	4	102
21	$\lambda/2$	79.10	2009	4	98
22	$\lambda/2$	75.90	1928	4	94
23	$\lambda/2$	72.70	1846	4	90
24	$\lambda/2$	69.50	1765	4	86
25	$\lambda/2$	66.30	1684	4	82
26	$\lambda/2$	63.10	1603	4	78
27	$\lambda/2$	59.90	1521	4	74
28	$\lambda/2$	56.70	1440	4	70
29	$\lambda/2$	53.50	1359	4	66
30	$\lambda/2$	50.30	1278	4	62
31	$\lambda/2$	47.10	1196	4	58
32	$\lambda/2$	43.90	1115	4	54
33	$\lambda/2$	40.70	1034	4	50
34	$\lambda/2$	37.50	952	4	46
35	$\lambda/2$	34.30	871	4	42
36	$\lambda/2$	31.10	790	4	38
37	$\lambda/2$	27.90	709	4	34
38	$\lambda/2$	24.70	627	4	30
39	$\lambda/2$	21.50	546	4	26
40	$\lambda/2$	18.30	465	4	22
41	$\lambda/2$	15.10	383	4	18
42	$\lambda/2$	11.90	302	4	14
43	$\lambda/2$	8.70	221	4	10
44	$\lambda/2$	5.50	140	4	6
45	$\lambda/2$	2.30	58	4	2
46	$\lambda/4$	0.00	0	2	0

